Applied Catalysis B: Environmental 182 (2016) 469–475

Contents lists available at ScienceDirect

Applied Catalysis B: Environmental

journal homepage: www.elsevier.com/locate/apcatb

Synthesis of niobium oxide nanoparticles with plate morphology utilizing solvothermal reaction and their performances for selective photooxidation

Kazuki Tamai [a], Saburo Hosokawa [a,b,*], Kentaro Teramura [a,b], Tetsuya Shishido [b,c], Tsunehiro Tanaka [a,b,*]

[a] Department of Molecular Engineering, Graduate School of Engineering, Kyoto University, Kyotodaigaku Katsura, Nishikyo-ku, Kyoto 615-8510, Japan
[b] Elements Strategy Initiative for Catalysts & Batteries (ESICB), Kyoto University, Kyotodaigaku Katsura, Nishikyo-ku, Kyoto 615-8245, Japan
[c] Department of Applied Chemistry, Graduate School of Urban Environmental Sciences, Tokyo Metropolitan University, 1-1 Minami-Osawa, Hachioji, Tokyo 192-0397, Japan

ARTICLE INFO

Article history:
Received 21 August 2015
Received in revised form
26 September 2015
Accepted 1 October 2015
Available online 9 October 2015

Keywords:
Photocatalyst
Selective photooxidation
Solvothermal synthesis
Nanoparticles

ABSTRACT

Nb_2O_5 composed of nano-plate particles with the width of ~35 nm and the length of ~200 nm can be readily synthesized from the nanocrystalline niobium compound intercalating ethylene glycol obtained by the solvothermal reaction of niobium ethoxide in ethylene glycol. Thus-obtained Nb_2O_5 nanoparticles have higher surface area and also higher catalytic activities of selective photooxidation of benzyl alcohol than Nb_2O_5 synthesized from $Nb_2O_5 \cdot nH_2O$. We conclude that the crystallinity and surface area of Nb_2O_5 are responsible to adsorption of the substrate, and the catalytic activities obviously correlate with the amount of substrate adsorbed on nanocrystalline Nb_2O_5.

1. Introduction

Niobium materials are of great interest in the field of environment related catalysts such as photocatalyst and solid acid catalyst [1–3]. Niobium oxide has an excellent catalytic ability for the photodecomposition of water as well as the photocatalytic transformation of organic compound [4–6]. Recently, $Nb_2O_5 \cdot nH_2O$ has been reported to work as water-tolerant heterogeneous Lewis acid and also to act as much effective catalyst for conversion of glucose into 5-(hydroxymethyl) furfural in water [7]. These catalytic performances are known to be responsible for the physical properties of catalyst such as particle size, surface area, crystallinity, and morphology.

The synthesis of Nb_2O_5 nanoparticles has been actively investigated by using various methods such as hydro- and solvo-thermal methods and sol–gel method, and so on [8–10]. In the course of our studies on the synthesis of metal oxide nanoparticles by a solvothermal method in organic media, inorganic-organic composites prepared by the solvothermal method in glycol have been found to be effective precursors for the synthesis of rare earth oxide nanoparticles such as CeO_2 or Y_2O_3 [11,12]. Furthermore, we have found that the pore structure or surface area of CeO_2 nanoparticles can be controlled by the choice of reaction conditions such as reaction temperature or solvent in the solvothermal method [13,14]. Thus, we have aimed to reveal explicitly the relation of physical properties of catalysts and their catalytic activities.

On the basis of such backgrounds, we have engaged in the study of novel synthesis of Nb_2O_5 nanoparticles by using the solvothermal reaction in ethylene glycol and their catalytic activities in the photooxidation of benzyl alcohol. The present study provides the following remarkable observations. (1) A layered niobium compound intercalating ethylene glycol, which has plate-like morphology, can be readily synthesized by a solvothermal method. (2) Significantly, the niobium compound is transformed into Nb_2O_5 (~35 nm in the width, ~200 nm in the length) maintaining the plate-like morphology. (3) Thus-obtained Nb_2O_5 nano-plate parti-

* Corresponding authors at: Department of Molecular Engineering, Graduate School of Engineering, Kyoto University, Kyotodaigaku Katsura, Nishikyo-ku, Kyoto 615–8510, Japan. Fax: +81 75 383 2561.
E-mail addresses: hosokawa@moleng.kyoto-u.ac.jp (S. Hosokawa), tanakat@moleng.kyoto-u.ac.jp (T. Tanaka).

http://dx.doi.org/10.1016/j.apcatb.2015.10.003
0926-3373/

cles have a high surface area which definitely correlates with high photocatalytic activity for benzyl alcohol photooxidation.

2. Experimental methods

2.1. Solvothermal synthesis

Niobium (V) ethoxide ($Nb(OC_2H_5)_5$) and ethylene glycol (EG) were purchased from Wako Co., Ltd. (Japan) and used without further purification. Solvothemral method was carried out by the following procedure. Niobium (V) ethoxide (10 g, 31 mmol) was suspended in 100 mL of EG in a test tube serving as an autoclave liner. The tube was placed in 330-mL autoclave. The autoclave was completely purged with nitrogen, heated to 573 K at the rate of 2.3 K min^{-1}, and kept at that temperature for two hours. The product was washed with methanol by vigorously mixing and centrifuging several times. Niobium oxides were synthesized by calcining the precursor at prescribed temperature for 30 min in a dry air flow. For comparison, niobium oxide hydrate ($Nb_2O_5{\cdot}nH_2O$, AD/3459, HY-340), which was kindly supplied from CBMM, was used as a starting material. Niobium oxides were similarly synthesized by calcination of $Nb_2O_5{\cdot}nH_2O$ under the conditions described above. In this paper, the products obtained from the solvothermal method and $Nb_2O_5{\cdot}nH_2O$ are designated as NbEG and NbOH, respectively. The abbreviation is followed by calcination temperature; for instance, NbEG-773 refers to the product obtained by calcination at 773 K of NbEG.

2.2. Photocatalytic reaction

Photocatalytic reactions were carried out in a batch system under an oxygen atmosphere (1 atm) using a gas bag. The reactor was equipped with an optically polished flat Pyrex glass cap. Niobium oxide catalysts (25 mg), benzyl alcohol (0.5 mmol), and toluene (2 mL) were introduced into the reactor. The catalysts were used without any pretreatments. The suspension was stirred by a magnetic stirrer at room temperature for 30 min in dark. Subsequently, light irradiation was performed from the top of the reactor with a 200 W Hg-Xe lamp (UVF-204S C-type, SAN-EI ELECTRIC, Japan) through UV-39 cut-off filter to shadow light below 370 nm which leads to photoexcitation from valence band to conduction band of Nb_2O_5. Reaction products were analyzed by FID-GC (GC-2014 AFsc) (Shimadzu, Japan) and GC mass spectrometry (GCMS-QP2010 Ultra) (Shimadzu, Japan).

2.3. Characterization

N_2 adsorption measurement was performed on a Belsorp-miniII (BEL, Japan) at 77 K. The specific surface area (*S*BET) was estimated from the N_2 adsorption isotherm using Brunauer–Emmett–Teller (BET) method. X-ray diffraction (XRD) measurement was carried out using a Rigaku Ultima IV X-ray diffractometer with Cu-Kα radiation (λ = 1.5406 Å). Simultaneous thermogravimetric and differential thermal analyses (TG-DTA) were performed on a TG 8120G thermal analyzer (Rigaku, Japan) from room temperature to 1273 K at a heating rate of 10 K min^{-1} in 80 mL min^{-1} flow of dry air. FT-IR spectra were obtained using a FT/IR-4200 (JASCO, Japan) with a resolution of 4 cm^{-1}. Solid samples were measured by KBr method in a transmission mode, and liquid phase ethylene glycol and niobium ethoxide were measured by binding with KBr plates. Morphologies of the samples were observed using a transmission electron microscope (TEM) (JEM-1400 or JEM-2010, JEOL, Japan). The adsorption experiments were conducted in the following procedures. Nb_2O_5 with or without pretreatment at 473 K under nitrogen flow (100 mL min^{-1}) and 5 mL cyclohexane solution containing benzyl alcohol (5 mM) were introduced into a vial and stirred for 5 h at 293 K. Then, the solution was filtered and benzyl alcohol concentration of the supernatant was determined with the absorbance at 290 nm of benzyl alcohol measured by UV–vis spectrometer (MCPD-7700), (Otsuka electronics, Osaka, Japan). The Nb K-edge X-ray absorption fine structure (XAFS) spectra were recorded in a transmission mode in air at room temperature using the facility of the BL01B1 beam line at SPring-8 of the Japan Synchrotron Radiation Research Institute. A Si (311) two-crystal monochromator was used to obtain a monochromatic X-ray beam. The data reduction was performed by the REX2000 program (Rigaku, Japan).

3. Results and discussion

3.1. Properties of solvothermally-synthesized product

3.1.1. XRD and TEM image

XRD pattern of solvothermally-synthesized product (NbEG) shows several peaks as shown in Fig. 1a, but these peaks are not due to those of reported niobium oxides which are in thermally stable phases such as pseudohexagonal (TT-Nb_2O_5), orthorhombic (T-Nb_2O_5) or monoclinic Nb_2O_5 (H-Nb_2O_5) [2]. It should be noted that NbEG has the intense peak at low angle (<10°, 8.2° in NbEG), the peak position of which is known to depend on the carbon number of intercalating primary alcohols or 1,ω-glycols [15,16]. The lattice spacing (10.8 Å) calculated from the peak position is nearly consistent with those of layered compounds intercalating ethylene glycol previously reported by other groups [17–22]. Considering these facts, NbEG obtained here must have a similar layered structure containing ethylene glycol moieties. As shown in Fig. 1b, the NbEG is composed of the plate-like particles with the width of ~50 nm and the length of ~200 nm.

3.1.2. EXAFS

Extended X-ray absorption fine structure (EXAFS) oscillations are shown in Fig. 1c. Remarkably, the EXAFS oscillation of NbEG in the range of 8–16 $Å^{-1}$ was similar with that of TT-Nb_2O_5. In the FT spectra, the peaks due to Nb–Nb oscillation in range from 3 Å to 4 Å were also consistent with those of TT-Nb_2O_5 (Fig. 1d). These results suggest that the local structure of Nb atoms in NbEG reflects the coordination structure surrounded by Nb atoms in TT-Nb_2O_5. In other words, the layer structure of NbEG is constructed by niobium oxide (NbO_x) with TT-Nb_2O_5-like structure.

3.1.3. FT-IR spectra

To investigate the state of organic species in NbEG, FT-IR spectra were measured (Fig. 2). Niobium ethoxide used as a starting material showed peaks at 2970, 2929, 2888 and 2861 cm^{-1} due to C—H stretching vibrations of ethoxy groups [23,24]. The peak at 2970 cm^{-1} due to CH asymmetric stretching vibration, that is, methyl group of ethoxy moiety, was not observed in NbEG (Fig. 2c). Instead, C—H stretching vibrations due to CH_2 group of ethylene glycol were observed at 2944, 2930, 2903, and 2873 cm^{-1}. Liquid ethylene glycol itself showed peaks also at around 2944 and 2877 cm^{-1} attributed to asymmetric and symmetric stretching vibrations of C—H bonds in methylene, respectively [25–27]. Characteristic absorption bands of NbEG in the region below 1500 cm^{-1} are also resemble with those of liquid ethylene glycol, but peaks at 1128 and 1115 cm^{-1} are obviously different from those of ethylene glycol. Since the C—O vibrations observed at around 1100 cm^{-1} are reported to split by complexation between metal ions and ethylene glycol [20–22,28], the splitting of C—O vibrations in NbEG suggests that ethylene glycol moieties are bounded with NbO_x layer. These results indicate that ethoxide groups around Nb atom are completely substituted to ethylene glycol. Characteristic absorption bands attributed to ethylene glycol in NbEG were sharper than

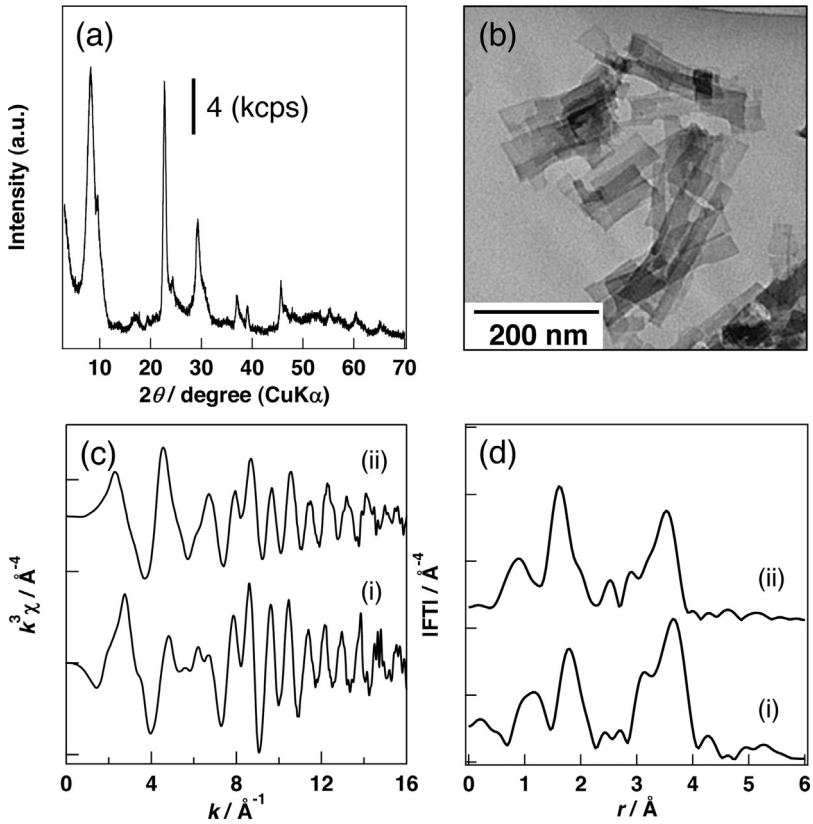

Fig. 1. XRD pattern and TEM image of NbEG (a and b). EXAFS oscillations and FT spectra (c and d) of NbEG (i) and TT-Nb_2O_5 (ii).

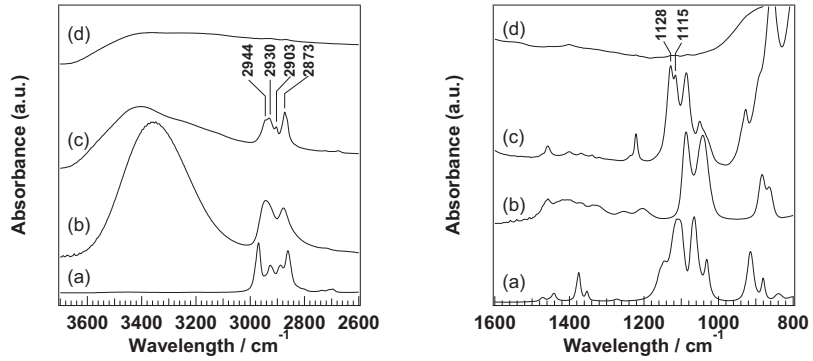

Fig. 2. FT-IR spectra of $Nb(OC_2H_5)_5$ (a), ethylene glycol (b), NbEG (c) and NbEG-623 (d).

those of liquid ethylene glycol. Similarly to this observation, solid ethylene glycol are known to show sharper absorption bands than liquid ethylene glycol [25,27]. Thus, ethylene glycol moieties in NbEG must be fixed between NbO_x layers.

3.1.4. TG-DTA

In the TG-DTA profile of NbEG shown in Fig. 3, a large weight loss associated with a sharp exothermic peak was detected at around 600 K, and the weight loss was about 22.3%. The product obtained by calcining at 623 K or 773 K did not show ethylene glycol moieties in the IR spectrum (Fig. 2d), and was TT-Nb_2O_5 corresponding to JCPDS card No. 28-317 in the XRD pattern (Figs. 4 e and 5 a). These results indicate that the ethylene glycol moieties in the NbO_x layers remove by combusting in air at around 600 K, resulted in the collapse of the layered structure. In XRD patterns (Fig. 4) of the calcined samples at around 600 K, peaks observed at low angle (<10°) gradually shifted to larger angle with the increase of calcina-

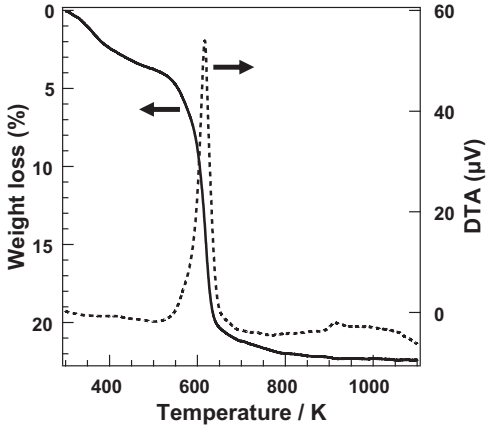

Fig. 3. TG-DTA of NbEG.

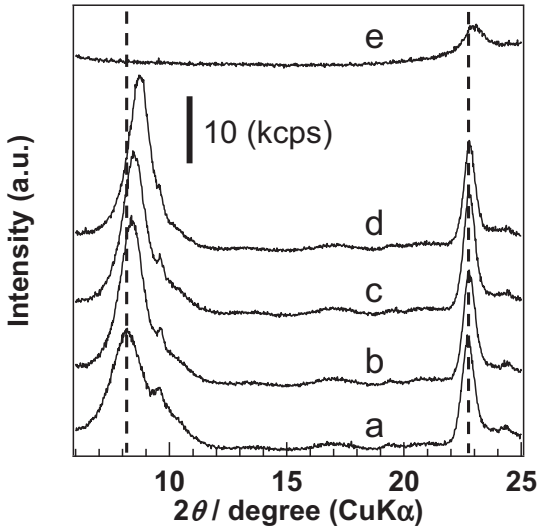

Fig. 4. XRD patterns of the products obtained by calcination of NbEG at various temperatures: as-synthesized product (a); 473 K (b); 523 K (c); 573 K (d); 623 K (e).

tion temperature, while the peak position observed at 22.8° were maintained regardless of the calcination temperature. These observations appear to correlate with the successive degradation of the ethylene glycol moieties at around 600 K. These results also suggest that a layered structure having the ethylene glycol moieties in the NbO_x layers is constructed by the solvothermal reaction of niobium ethoxide in ethylene glycol.

3.2. Properties of calcined samples

Table 1 summarizes physical properties of Nb_2O_5 synthesized from NbEG or NbOH. BET surface areas of Nb_2O_5 synthesized from NbEG were larger than those from NbOH. The surface areas, however, decreased with increasing calcination temperature and eventually physical properties of Nb_2O_5 obtained by calcination of NbEG at above 973 K were identical with those of NbOH at above 973 K. The crystal phase of Nb_2O_5 synthesized from NbEG was transformed from TT-Nb_2O_5 to T-Nb_2O_5 at 873 K, and the temperature was 973 K in the case of NbOH.

Fig. 5a shows XRD patterns of NbEG-773 and NbOH-773 obtained by calcination at 773 K of NbEG or NbOH, respectively. NbEG-773 had the peaks at 23.0 and 46.4° due to 001 and 002 planes of TT-Nb_2O_5, respectively, but no characteristic peak was detected in NbOH-773. TEM images revealed that NbEG-773 was mainly composed of plate-like particles with the width of ~35 nm and the length of ~200 nm, even though the aggregate formed by a collapse of the plate-like particle was partly observed. On the other hand, apparent aggregates of irregularly-shaped particles were observed in NbOH-773. The most remarkable point is that the morphology of NbEG-773 is almost the same with that of NbEG. High resolution TEM image in Fig. 5b indicated that NbEG-773 had lattice fringes (0.38 nm) of NbEG-773 corresponded to 001 plane of TT-Nb_2O_5. The selected area electron-diffraction (SAED) of NbEG-773 showed spots due to 001 plane of TT-Nb_2O_5. The SAED agreed well with the result obtained from XRD pattern. These results suggests that each plate-like particle of NbEG-773 has a single crystal nature of TT-Nb_2O_5. Of importance is that the transformation from NbEG to Nb_2O_5 aligns the orientation to *c* axis of crystallite of TT-Nb_2O_5.

3.3. Crystallization mechanism

A plausible crystallization mechanism of TT-Nb_2O_5 from NbEG is illustrated in Fig. 6. The mechanism includes the following three steps. (1) The layered niobium compound intercalating ethylene glycol (~50 nm in the width, ~200 nm in the length) is formed by the solvothermal reaction at 573 K in ethylene glycol. (2) The ethylene glycol moieties between NbO_x layers are eliminated at around 600 K during calcination process, resulting in the shrink of the interlayer in the niobium compound. (3) The niobium compound is completely transformed to TT-Nb_2O_5 nanoparticle having plate-

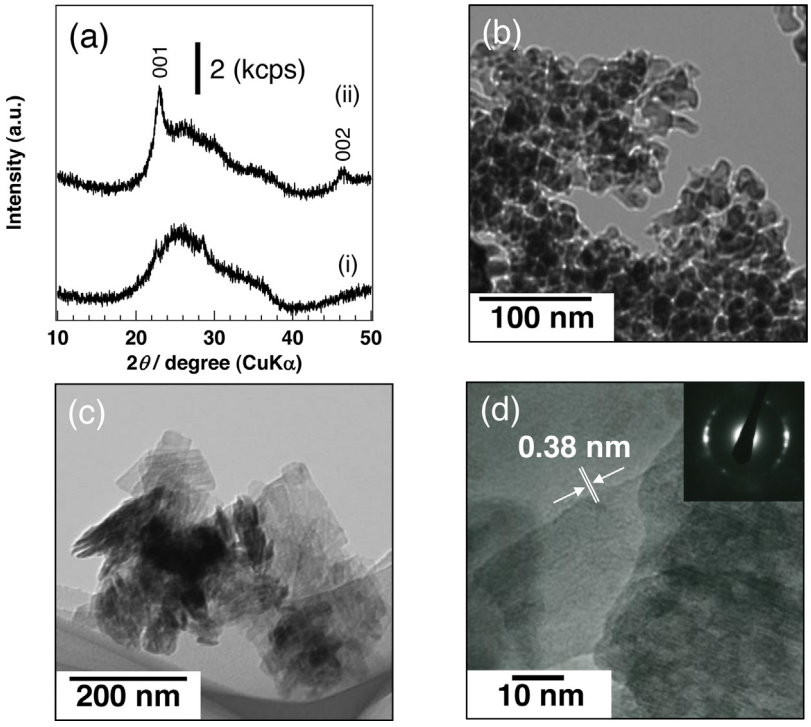

Fig. 5. (a) XRD patterns of NbOH-773 (i) and NbEG-773 (ii). TEM images of NbOH-773 (b) and NbEG-773 (c and d).

Table 1
Physical properties of niobium oxide synthesized from NbEG and NbOH.

	Calcination temp./K	Phase	BET surface area/$m^2 g^{-1}$	Crystallite size[a]/nm	Morphology
NbEG	673	TT[b]	146	–	Plate
	773	TT	113	–	Plate
	873	T	72	43	Plate
	973	T	24	74	Cylinder
	1073	T	9	110	Cylinder
NbOH	673	am	114	–	–
	773	am	86	–	–
	873	TT	40	42	Sphere
	973	T	17	64	Cylinder
	1073	T	8	120	Cylinder

[a] The crystallite size was calculated from the half-height width of the peak due to 001 plane by Scherrer's equation.
[b] The abbreviations are as follows; am, amorphous phase; TT, TT-Nb_2O_5; T, T-Nb_2O_5.

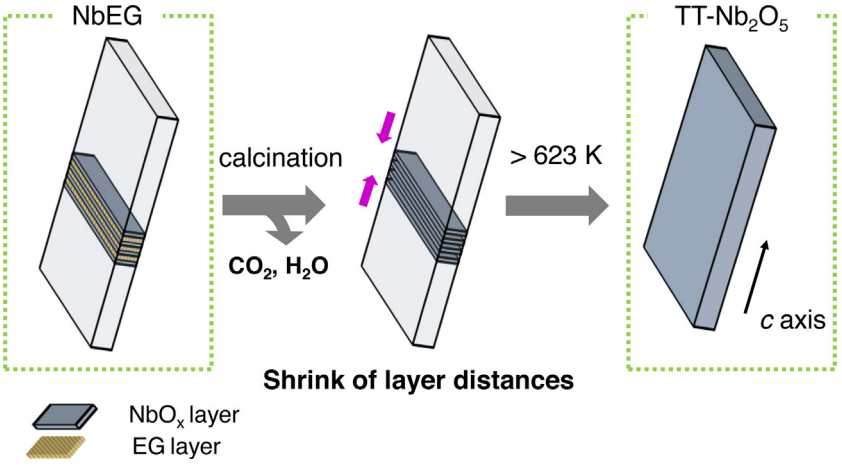

Fig. 6. Crystallization mechanism from NbEG to TT-Nb_2O_5.

like morphology at 623 K with maintenance of the morphology of the nanocrystalline layered niobium compound.

Considering the crystallization mechanism, the morphology of nanocrystalline niobium compound with layered structure is important in terms of the morphology control of TT-Nb_2O_5. Actually, the niobium compound prepared by solvothermal reaction at 523 K, a lower temperature than usual, resulted in poor layered structure, and the product obtained by calcination at 773 K was TT-Nb_2O_5 without the preferential orientation to *c* axis (Fig. 7).

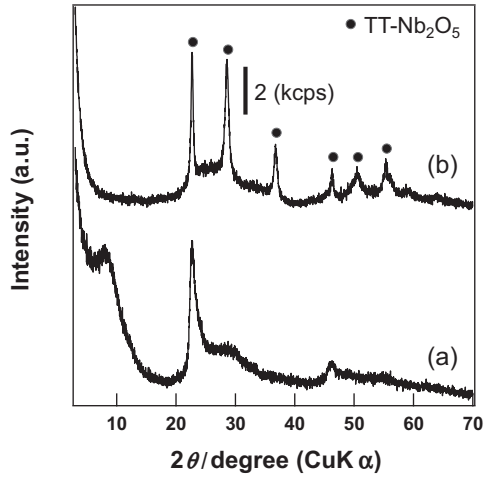

Fig. 7. XRD patterns of niobium compound prepared by solvothermal reaction at 523 K (a) and the product obtained by the calcination at 773 K of the niobium compound (b).

To the best of our knowledge, there has been so far no report on the synthesis of the well-crystallized niobium compounds intercalating ethylene glycol, although the reaction in ethylene glycol of niobium ethoxide or chloride has been reported to yield amorphous products with microporous structure or ethylene glycol-modified niobium hydroxide [29,30]. Thus, we would like to emphasize that the present paper provides the first demonstration that the nanocrystalline layered niobium compound intercalating ethylene glycol can be synthesized by the solvothermal method, and thus obtained compounds are able to be transformed into TT-Nb_2O_5 maintaining its plate-like morphology.

3.4. Selective photooxidation of benzyl alcohol

Selective photooxidation of various organic compounds has been known to proceed over Nb_2O_5 with visible light through an unique photoexcitation mechanism between conduction band of Nb_2O_5 and donor levels generated by adsorption of substrates on Nb_2O_5 [5–6,31–34]. Actually, from DFT calculations in previous report [34], the alcoholate formed on Nb_2O_5 was confirmed to generate the donor levels over the valence band of Nb_2O_5 itself. The narrow energy gap permits photoexcitation with visible light (>390 nm) to proceed photooxidation of alcohols under visible light irradiation. The catalytic abilities of niobium oxides obtained in the present work were evaluated in the photooxidation of benzyl alcohol (BnOH). For all the catalysts benzaldehyde was the main product, and benzoic acid or carbon dioxide was scarcely detected in the present reaction conditions. The production amount of benzaldehyde linearly increased among the examined catalysts having different physical properties, and an induction period was hardly observed in early reaction period (Fig. S1). Therefore, the initial rate

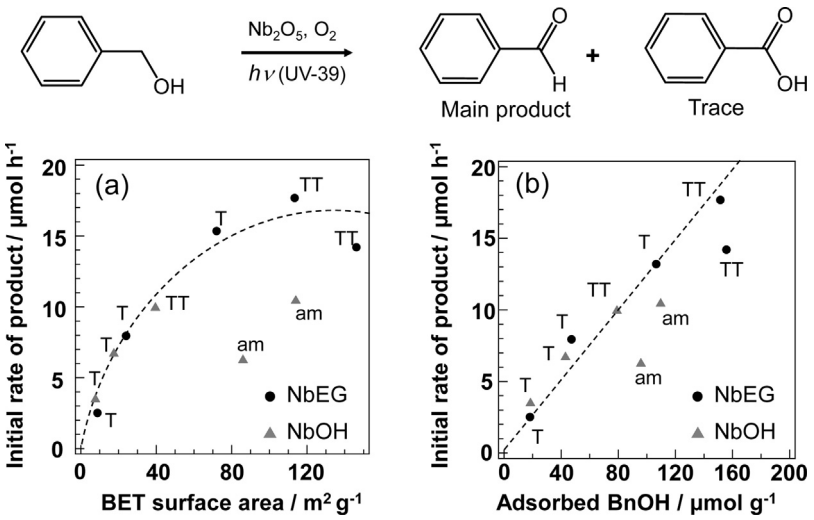

Fig. 8. Catalytic activity in the selective photooxidation of benzyl alcohol and the amount of benzyl alcohol (BnOH) adsorbed on various catalysts. The abbreviations are as follows; am, amorphous phase; TT, TT-Nb_2O_5; T, T-Nb_2O_5. The initial rate of benzaldehyde production vs BET surface area (a). The initial rate of benzaldehyde production vs the amount of adsorbed benzyl alcohol (BnOH) on various catalysts synthesized from NbEG and NbOH (b).

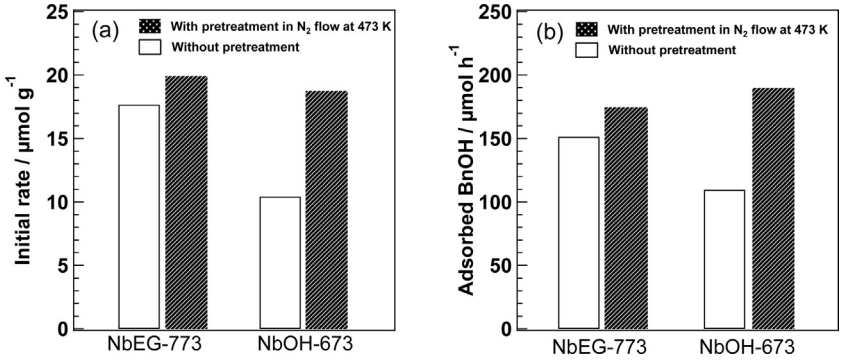

Fig. 9. (a) Selective photooxidation of benzyl alcohol where the catalytic activity was evaluated by the initial rate of benzaldehyde production. (b) The amount of adsorbed benzyl alcohol (BnOH) on NbEG-773 and NbOH-673 with or without the pretreatment in N_2 flow at 473 K. The surface area (104 $m^2\ g^{-1}$) of NbEG-773 was essentially identical with that (112 $m^2\ g^{-1}$) of NbOH-673 having amorphous phase.

of benzaldehyde production was used as an indicator of photocatalytic activities as shown in Fig. 8a. The initial rates of benzaldehyde production were calculated with slops of approximation straight lines (Fig. S1) obtained from several plots of benzaldehyde production in early reaction period in which the conversion of benzyl alcohol was below 5%. Nb_2O_5 synthesized from NbEG exhibited higher activities than those from NbOH, and the catalytic activities evidently correlated with the surface areas of the catalysts, except for TT-Nb_2O_5 (146 m^2/g) of NbEG-673 and amorphous ones. Previously, we have reported that the selective photooxidation of alcohol over Nb_2O_5 proceeds via the formation of a surface complex generated between alcohol and the surface of Nb_2O_5 [5,6]. The catalytic activity, therefore, must improve with increasing the surface area. In fact, the amount of adsorbed BnOH well correlated with the surface areas of nanocrystallized-Nb_2O_5, similarly to the catalytic activities (Fig. 8b). These findings suggest that the enlargement of the surface area of nanocrystalline-Nb_2O_5 improves the catalytic activity.

NbEG-673 and amorphous products derived from NbOH showed low catalytic activities regardless of their high surface areas. All Nb_2O_5 catalysts synthesized from NbEG were white powders except for NbEG-673 which colored into pale gray. NbEG-673 is considered to contain a small amount of charred remains of ethylene glycol moieties. This result is also supported by the TG analysis of NbEG (Fig. 3), suggesting that the carbon species inhibit the adsorption of BnOH and the catalytic activity. In the case of amorphous products, the pretreatment at 473 K under nitrogen flow (100 mL min^{-1}) improved both the catalytic activity and the adsorption amount of BnOH (Fig. 9). These results imply that the active sites on the surface of amorphous niobium oxide are covered with adsorbents such as water molecules to inhibit the absorption of BnOH, thereby resulting in the decrease of the catalytic activity. If the catalytic activities and the amounts of adsorbed BnOH obtained in the pretreated amorphous products are added in Fig. 8b, these values agree with the linear relationship obtained in crystallized Nb_2O_5 catalysts. Thus, the crystallinity of Nb_2O_5, which must be responsible to adsorption of substrates, is crucial for the enhancement of catalytic activity.

4. Conclusions

In summary, TT-Nb_2O_5 nano-plate particles can be readily prepared with maintenance of the plate-like morphology from the layered niobium compound intercalating ethylene glycol obtained by the solvothermal method. The Nb_2O_5 photocatalysts prepared from the niobium compound have higher surface areas and also higher catalytic activities for the selective photooxidation of benzyl alcohol, compared to those prepared from NbOH. The photocatalytic activities correlate with the surface areas of nanocrystallized-Nb_2O_5. The observations described herein could

provide not only an avenue of morphology control of metal oxides by utilizing the specificity of organic-inorganic composite, but also a clue for the enhancement of catalytic activity in various reactions using solid catalysts.

Acknowledgements

This work was supported in part by Grant-in-Aid for challenging Exploratory Research (26620193) from the Ministry of Education, Culture, Sports, Science and Technology and by the Program for Element Strategy Initiative for Catalysts & Batteries (ESICB). The X-ray absorption experiments were performed with the approval of the Japan Synchrotron Radiation Research Institute (JASRI) (Proposal No. 2014B1371).

Appendix A. Supplementary data

Supplementary data associated with this article can be found, in the online version, at http://dx.doi.org/10.1016/j.apcatb.2015.10.003.

References

[1] K. Tanabe, S. Okazaki, Appl. Catal. A 133 (1995) 191–218.
[2] I. Nowak, M. Ziolek, Chem. Rev. 99 (1999) 3603–3624.
[3] T. Okuhara, Chem. Rev. 102 (2002) 3641–3666.
[4] R. Abe, K. Shinohara, A. Tanaka, M. Hara, J.N. Kondo, K. Domen, Chem. Mater. 9 (1997) 2179–2184.
[5] T. Ohuchi, T. Miyatake, Y. Hitomi, T. Tanaka, Catal. Today 120 (2007) 233–239.
[6] T. Shishido, T. Miyatake, K. Teramura, Y. Hitomi, H. Yamashita, T. Tanaka, J. Phys. Chem. C 113 (2009) 18713–18718.
[7] K. Nakajima, Y. Baba, R. Noma, M. Kitano, J.N. Kondo, S. Hayashi, M. Hara, J. Am. Chem. Soc. 133 (2011) 4224–4227.
[8] H. Kominami, K. Oki, M. Kohno, S. Onoue, Y. Kera, B. Ohtani, J. Mater. Chem. 11 (2001) 604–609.
[9] T. Murayama, J. Chen, J. Hirata, K. Matsumoto, W. Ueda, Catal. Sci. Technol. 4 (2014) 4250–4257.
[10] M.A. Bizeto, V.R.L. Constantino, Eur. J. Inorg. Chem. (2007) 579–584.
[11] S. Hosokawa, S. Iwamoto, M. Inoue, Mater. Res. Bull. 43 (2008) 3140–3148.
[12] S. Hosokawa, S. Iwamoto, M. Inoue, J. Alloys Compd. 457 (2008) 510–516.
[13] Y. Hayashi, S. Hosokawa, M. Inoue, Microporous Mesoporous Mater. 128 (2010) 115–119.
[14] S. Hosokawa, K. Shimamura, M. Inoue, Mater. Res. Bull. 46 (2011) 1928–1932.
[15] M. Inoue, M. Kimura, T. Inui, Chem. Mater. 12 (2000) 55–61.
[16] M. Inoue, H. Kominami, T. Inui, J. Chem. Soc. Dalton Trans. (1991) 3331–3336.
[17] M. Inoue, Y. Kondo, T. Inui, Inorg. Chem. 27 (1988) 215–221.
[18] A. Kasai, S. Fujihara, Inorg. Chem. 45 (2006) 415–418.
[19] Y. Xi, R.J. Davis, Inorg. Chem. 49 (2010) 3888–3895.
[20] X. Wang, Y. Yang, T. Zhai, Y. Zhong, Z. Gu, Y.C. Cao, Y. Zhao, Y. Ma, J. Yao, Chem. Eur. J. 19 (2013) 5442–5449.
[21] V.N. Krasil'nikov, O.I. Gyrdasova, I.V. Baklanova, L.Y. Buldakova, M.Y. Yanchenko, R.F. Samigullina, O.V. Koryakova, Russ. J. Inorg. Chem. 58 (2) (2013) 120–126.
[22] S. Kikkawa, F. Kanamaru, M. Koizumi, Inorg. Chem. 19 (1980) 259–262.
[23] Y. Cai, S. Yang, S. Jin, H. Yang, G. Hou, J. Xia, J. Cent. S. Univ. Technol. 18 (2011) 73–77.
[24] G.A. Pitsevich, I.Y. Doroshenko, V.E. Pogorelov, V. Shablinskas, V. Balevichus, E.N. Kozlovskaya, Am. J. Chem. 2 (4) (2012) 218–227.
[25] H. Takeuchi, M. Tasumi, Chem. Phys. 77 (1983) 21–34.
[26] H. Matsuura, M. Hiraishi, T. Miyazawa, Spectrochim. Acta 28A (1972) 2299–2304.
[27] H. Matsuura, T. Miyazawa, Bull. Chem. Soc. Jpn. 40 (1967) 85–94.
[28] R.S. Ghadwal, R.C. Mehrotra, A. Singh, Transition Met. Chem. 30 (2005) 836–844.
[29] D. Khushalani, G.A. Ozin, A. Kuperman, J. Mater. Chem. 9 (1999) 1491–1500.
[30] S. Sarina, H. Zhu, Z. Zheng, S. Bottle, J. Chang, X. Ke, J. Zhao, Y. Huang, A. Sutrisno, M. Willans, G. Li, Chem. Sci. 3 (2012) 2138–2146.
[31] S. Furukawa, T. Shishido, K. Teramura, T. Tanaka, J. Phys. Chem. C 115 (2011) 19320–19327.
[32] S. Furukawa, Y. Ohno, T. Shishido, K. Teramura, T. Tanaka, J. Phys. Chem. C 117 (2013) 442–450.
[33] S. Furukawa, T. Shishido, K. Teramura, T. Tanaka, ChemPhysChem 15 (2014) 2665–2667.
[34] S. Furukawa, Y. Ohno, T. Shishido, K. Teramura, T. Tanaka, ChemPhysChem 12 (2011) 2823–2830.